

Electron-energy-loss study of the space-charge region at semiconductor surfaces

L. H. Dubois and B. R. Zegarski
AT&T Bell Laboratories, Murray Hill, New Jersey 07974

B. N. J. Persson
Institut für Festkörperforschung der Kernforschungsanlage, D-5170 Jülich, West Germany
 (Received 7 November 1986)

We derive a simple but general formula which describes the width of the quasielastic peak in inelastic electron scattering from doped semiconductors and which is used to analyze the space-charge region at the GaAs(100) surface. The analysis shows that the Fermi level at the surface is pinned 0.8 eV below the conduction-band edge in the absence of any metal or oxide overlayer and that the free-carrier concentration in the near-surface region can be readily reduced from the bulk value. This reduction is caused by the surface preparation (sputtering and annealing) which introduces acceptor point defects in this region of the GaAs crystal.

I. INTRODUCTION

Considerable interest exists in the near-surface properties of semiconductor crystals. It has recently been demonstrated that useful information about the space-charge region and the Fermi-level pinning position can be obtained from high-resolution electron-energy-loss (EELS) measurements. Thus in the work by Matz and Lüth¹ and by Dubois and Schwartz,² information about the space-charge layer at GaAs surfaces was deduced from a study of the variation of the surface-plasmon frequency with bulk doping level. In many cases, however, it is difficult to resolve the low-energy surface-plasmon resonance due to the tailing of the elastic scattering peak. In other cases, e.g., for Si, the surface plasmon is overdamped and does not give rise to a sharp peak in the loss spectrum. Recently, however, Strocio and Ho³ were able to probe the space-charge region at the Si(111)-(7×7) surface by studying the temperature dependence of the width of the quasielastic peak. Indeed, this latter approach constitutes a very general and accurate method for probing the space-charge region of any semiconductor surface. The only requirement is that the surface-plasmon resonance frequency be much smaller than the width of the quasielastic peak which, of course, can be satisfied by working with lightly doped semiconductor crystals.

It is the aim of the present work to carry the study of Strocio and Ho³ further by deriving a simple but general formula which describes the temperature dependence of the width of the quasielastic peak. As an illustration, we present an analysis of experimental data obtained for GaAs(100) which shows that the Fermi level at the surface is pinned 0.8 eV below the conduction-band edge. In addition, we demonstrate that the free-carrier concentration in the vicinity of the surface can be readily manipulated by sputtering and annealing the sample. This procedure introduces acceptor traps in the near-surface region of the GaAs crystal which can compensate the excess charge from *n*-type dopants.

II. THEORY

The dielectric function of a homopolar semiconductor such as Si can, when $\hbar\omega \ll E_g$ (where E_g is the band gap), be written as

$$\epsilon(\omega) = \epsilon_0 - \frac{\omega_p^2}{\omega(\omega + i/\tau)}, \quad (1)$$

where ϵ_0 is the contribution from interband transitions. The plasmon frequency ω_p and the Drude relaxation time τ can be related to the free-carrier concentration n , the effective mass m^* , and the mobility μ via

$$\omega_p^2 = 4\pi n e^2 / m^*, \quad (2)$$

$$\tau = \mu m^* / e. \quad (3)$$

For a polar semiconductor such as GaAs there will be an additional contribution to the dielectric function from optical phonons:

$$\epsilon(\omega) = \epsilon_\infty + \frac{(\epsilon_0 - \epsilon_\infty)\omega_{TO}^2}{\omega_{TO}^2 - \omega^2 - i\omega\Gamma} - \frac{\omega_p^2}{\omega(\omega + i/\tau)}. \quad (4)$$

For most polar semiconductors $\omega_{TO} \sim 30$ meV, so that if we study the quasielastic peak for, say $|\omega| < 10$ meV, then (4) reduces to (1) to a good approximation, i.e., the optical phonons are not directly involved except that they give a contribution $(\epsilon_0 - \epsilon_\infty)$ to the static dielectric function.

Most semiconductor surfaces have a large density of states occurring in the bulk band gap. These surface states either are intrinsic⁴ or caused by impurities (e.g., adsorbed gases) and/or lattice imperfections (e.g., steps or vacancies) at the surface. In either case, the Fermi level will be pinned at the surface. The mobile carriers will then rearrange themselves in the surface region of the semiconductor crystal in such a way as to set up an electrostatic potential which bends the valence and conduction bands in the vicinity of the surface, making the Fer-

mi level equal everywhere [see Fig. 1(a)]. In the so-called depletion-layer approximation, one assumes that a layer of thickness W exists at the surface which is fully depleted of free carriers [see Fig. 1(b)]. By solving Poisson's equation, one can easily show that⁵

$$W = (\epsilon_0 \phi / 2\pi n e^2)^{1/2}, \quad (5)$$

where ϕ is the surface potential energy barrier [see Fig. 1(a)]. Within this model, the dielectric properties of the semiconductor crystal are represented by those of a uniform slab with dielectric constant ϵ_0 and thickness W in contact with a semi-infinite substrate with a dielectric function given by Eq. (1).

Assume now that a monochromatic beam of electrons (energy E_0 and angle of incidence α) is incident on the crystal. In the so-called dipole scattering theory,⁶ which always gives the dominant contribution to the scattering cross section for small loss energies,⁷ the single scattering "probability" $P_s(\omega)$ is given by⁷

$$P_s(\omega) = \frac{2}{(ea_0\pi)^2} \frac{1}{k^2 \cos\alpha} \frac{v}{\omega} \times \int_0^\infty dx \frac{1}{x} f(x, \alpha) \text{Im}g(\omega(x/v), \omega), \quad (6)$$

where

$$f(x, \alpha) = \frac{1}{x} \int_0^{2\pi} d\psi \left[1 + \left[\frac{1/x}{\cos\alpha} - \tan\alpha \cos\psi \right]^2 \right]^{-2}. \quad (7)$$

In this expression, a_0 is the Bohr radius, $E_0 = \hbar^2 k^2 / 2m = mv^2 / 2$ is the kinetic energy of the incident electrons, and $\text{Im}g(q_{\parallel}, \omega)$ is a linear-response function which describes the energy absorption in the medium.^{7,8} For the three-layer model described above (vacuum-depletion layer-substrate), Mills has shown that⁹

$$\text{Im}g = -2 \text{Im} \frac{1}{1 + \bar{\epsilon}}, \quad (8)$$

where

$$\bar{\epsilon} = \epsilon_0 \frac{1 + \Delta \exp(-2q_{\parallel} W)}{1 - \Delta \exp(-2q_{\parallel} W)} \quad (9)$$

and

$$\Delta = \frac{\epsilon - \epsilon_0}{\epsilon + \epsilon_0} = \frac{\bar{\omega}^2}{\bar{\omega}^2 - \omega(\omega + i/\tau)}, \quad (10)$$

where $\bar{\omega} = \omega_p / \sqrt{2\epsilon_0}$.

The scattering probability, $P_s(\omega)$, only accounts for single scattering, i.e., the incident electron is assumed to scatter inelastically from the substrate at most once. The full multiple scattering probability $P(\omega)$ can be obtained directly from $P_s(\omega)$ as has been shown elsewhere.^{7,10} In particular, the second moment

$$\langle (\Delta\omega)^2 \rangle = \langle (\omega - \langle \omega \rangle)^2 \rangle,$$

where

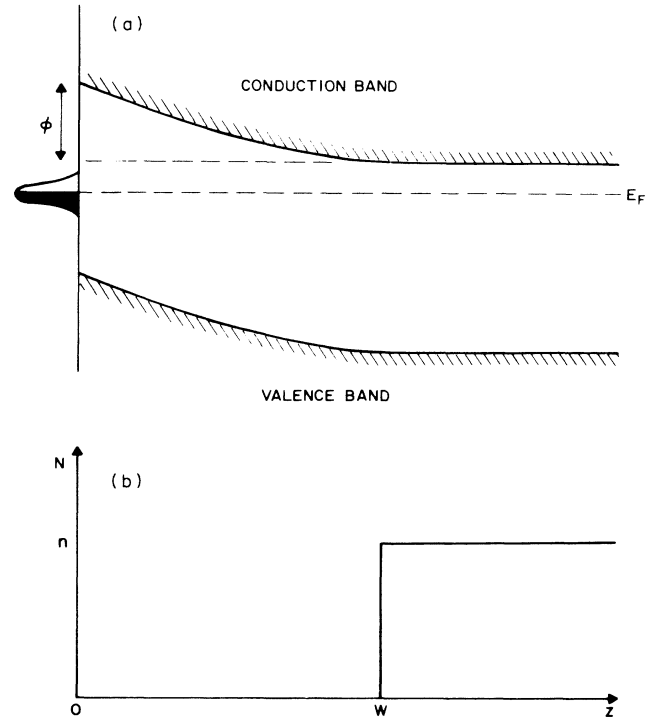


FIG. 1. (a) Band bending at a semiconductor surface; ϕ is the barrier height. (b) The free-carrier concentration $n(z)$ in the depletion-layer approximation. W is the width of the depletion layer; $n(z)=0$ for $0 < z < W$ and $n(z)=n$ for $z > W$, where n is the bulk free-carrier concentration.

$$\langle \omega \rangle = \int d\omega \omega P(\omega),$$

can be obtained from $P_s(\omega)$ via⁷

$$\langle (\Delta\omega)^2 \rangle = \int d\omega 2\omega^2 n_\omega P_s(\omega). \quad (11)$$

[Here, we have neglected a temperature-independent contribution to $\langle (\Delta\omega)^2 \rangle$ which is of no direct interest in the

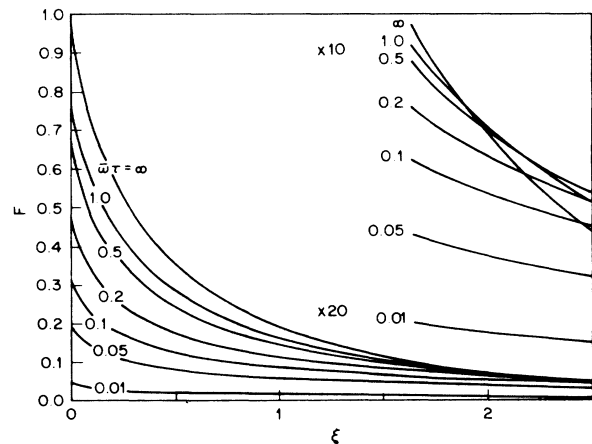


FIG. 2. The function F [see Eq. (14)]. The angle of incidence $\alpha = 60^\circ$.

present context.]

We now assume that the temperature is so high (or alternatively that the loss energy $\hbar\omega$ is so small) that we can approximate the Bose-Einstein factor n_ω by its high-temperature limit

$$n_\omega = [\exp(\hbar\omega/k_B T) - 1]^{-1} \approx k_B T / \hbar\omega. \quad (12)$$

Substituting Eqs. (6)–(10) and (12) in (11) gives, after

$$F = \frac{4\sqrt{2}}{\pi^3} \frac{\sqrt{\epsilon_0(\epsilon_0+1)}}{\epsilon_0-1} \frac{1}{\cos\alpha} \int_0^\infty dx \frac{1}{x} f(x, \alpha) \int_0^\infty dy \frac{\frac{\epsilon_0+1}{\epsilon_0-1} \frac{y}{\bar{\omega}\tau} e^{-xy\xi}}{\left[\frac{\epsilon_0+1}{\epsilon_0-1} (1-y^2) + e^{-xy\xi} \right]^2 + \left[\frac{\epsilon_0+1}{\epsilon_0-1} \frac{y}{\bar{\omega}\tau} \right]^2}, \quad (14)$$

where

$$\xi = \left(\frac{2\phi}{E_0} \frac{m}{m^*} \right)^{1/2}. \quad (15)$$

In principle, F depends not only on α , $\bar{\omega}\tau$, and ξ but also on ϵ_0 . This dependence is so weak, however, that it can be neglected (F fluctuates only a few percent as ϵ_0 changes from $3 \rightarrow \infty$). The function F is shown in Fig. 2 for $\alpha=60^\circ$. Equation (13), together with the curves in Fig. 2, are the main results of this section. In Sec. IV, we use this equation and Fig. 2 to analyze EELS data obtained from Si(111)-(7×7) and GaAs(100) surfaces.

III. EXPERIMENTAL PROCEDURE

The high-resolution electron-energy-loss spectrometer consists of two 127° cylindrical sectors similar to the design of Sexton.¹¹ The angle and energy of the incident electron beam were held fixed at 60° and 5 eV, respectively, and only electrons scattered within $\sim 1.5^\circ$ of the specular direction were collected. Typical maximum count rates were 5×10^4 counts/sec with an overall resolution of 5.5 meV (full width at half maximum of the elastic-scattering peak). The spectrometer was housed in a diffusion and titanium sublimation-pumped ultrahigh vacuum (UHV) chamber which was operated at $(1-2) \times 10^{-10}$ Torr during data collection.

Polished, Te-doped ($8 \times 10^{16} \text{ cm}^{-3}$) (100)-oriented GaAs wafers were obtained from Cambridge Instruments and etched in 1:1 HF:H₂O prior to introduction into the ultrahigh vacuum chamber. Approximately 1-cm² samples were cut from the center of the wafer and mounted on a small temperature-controlled molybdenum block. Samples could be heated to over 1000 K by a noninductively wound filament or cooled to 120 K via copper braids attached to a small liquid-nitrogen reservoir. Clean surfaces were prepared by 500-eV neon-ion bombardment at room temperature followed by annealing at ~ 850 K. Preparation conditions are discussed in the next section.

some simplification, the linewidth Γ [full width at half maximum (*FWHM*); the line profile is assumed to be a Gaussian so that $\Gamma^2 = 8 \ln 2 \langle (\Delta\omega)^2 \rangle$]:

$$\Gamma^2 = 128.6 \frac{k_B T \hbar\omega_{sp}}{(\epsilon_0+1) \cos\alpha \sqrt{E_0}} F(\alpha, \bar{\omega}\tau, \xi). \quad (13)$$

$\hbar\omega_{sp}$ and $\hbar\omega_p / \sqrt{\epsilon_0+1}$ and E_0 is measured in electron volts,

Surface cleanliness and order were routinely checked by Auger electron spectroscopy and low-energy electron diffraction (LEED) prior to performing the EELS measurements.

Sample temperatures were measured using a Cr-Al thermocouple pressed against the front surface of the crystal with a tantalum spring clip. The temperature did not vary more than ± 1 K during the recording of each EELS spectrum. The quasielastic peak full width at half maximum could be measured to within 0.2 meV; the measured results were reproducible to within 1 meV.

IV. RESULTS AND DISCUSSION

Before analyzing our new experimental data, let us briefly consider the results of Stroschio and Ho³ on Si(111)-(7×7). They performed EELS measurements on As-doped silicon crystals ($n = 6.6 \times 10^{12}$, 8.9×10^{15} , and $5.6 \times 10^{16} \text{ cm}^{-3}$) over a large temperature interval $40 < T < 900$ K. Here, we focus on only the $T=300$ -K data. The width of the quasielastic peak from an essentially undoped ($n = 6.6 \times 10^{12} \text{ cm}^{-3}$) Si crystal was found to be 13.9 meV. For the $n = 5.6 \times 10^{16} \text{ cm}^{-3}$ crystal, they found the linewidth to be 19.4 meV. Hence, assuming that both peak profiles are well approximated by Gaussians, the instrumental contribution to the linewidth can be removed by

$$\Gamma^2 = 19.4^2 - 13.9^2 = 183 \text{ meV}^2. \quad (16)$$

For $n = 5.6 \times 10^{16} \text{ cm}^{-3}$, $\epsilon_0 = 11.7$, and the effective mass $m^* = 0.26m_e$, we determine that

$$\hbar\omega_{sp} = 4.8 \text{ meV}. \quad (17)$$

Substituting these values into Eq. (13) with $E_0 = 6.8$ eV and $\alpha = 60^\circ$ gives $F = 0.19$. The mobility of electrons in Si at $T = 300$ K is¹² $\sim 850 \text{ cm}^2/\text{V sec}$ so that

$$\tau = 1.26 \times 10^{-13} \text{ sec} \quad \text{and} \quad \bar{\omega}\tau = 0.64.$$

Using Fig. 2 with $F = 0.19$ and $\bar{\omega}\tau = 0.64$ gives $\xi = 0.74$

and from Eq. (15) we get $\phi = 0.48$ eV. The depletion layer thickness calculated from Eq. (5), 1040 Å, agrees well with both the results of Strosio and Ho³ (1050±150 Å) and with other experimental data [photoemission measurements show that the Fermi level is pinned 0.53 eV below the conduction-band edge at the Si(111)-(7×7) surface¹³].

Let us now turn to the somewhat more complicated, but also more interesting, case of GaAs(100). Figure 3 shows the temperature dependence of the full width at half maximum of the quasielastic peak from Te-doped ($8 \times 10^{16} \text{ cm}^{-3}$) GaAs(100). This sample was prepared by mild sputtering followed by annealing at 850 K for 60 min. At room temperature the measured width is on the order of 14 meV so that

$$\Gamma^2 = 14^2 - 5.5^2 = 168 \text{ meV}^2. \quad (18)$$

Using an analysis identical to that for silicon except with $\epsilon_0 = 12.85$ and $m^* = 0.067m_e$, one finds that $F = 0.062$. The measured mobility of our sample is $4180 \text{ cm}^2/\text{V sec}$ so that $\bar{\omega}\tau$ becomes ≈ 1.9 . Using these values in Fig. 2, gives $\xi = 2.2$ and from Eq. (15) we get $\phi = 0.81$ eV. This value for the Fermi-level pinning position is very close to that measured by other techniques whether in the presence¹⁴ or absence^{15,16} of any metal overlayer (i.e., this is an intrinsic property of GaAs). We note that the GaAs(100) surface can form a large number of reconstructed phases of varying stoichiometry,¹⁷ but these in no way effect the results discussed here since we are probing the near-surface region of the sample ($10^3 - 10^4$ -Å deep⁶).

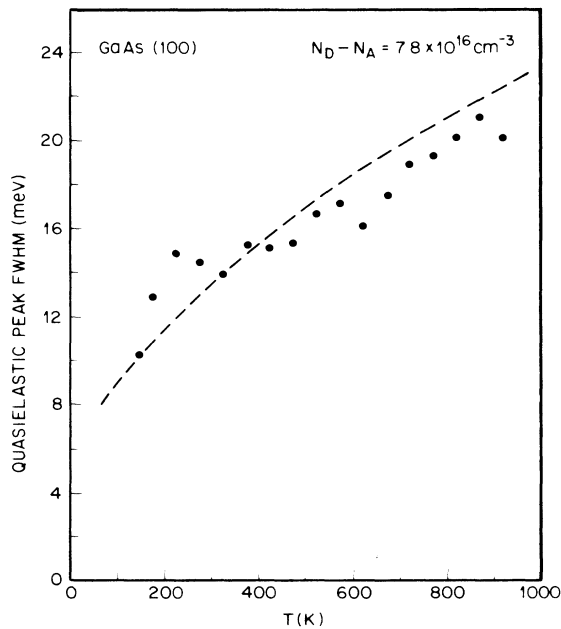


FIG. 3. The width of the quasielastic peak as a function of temperature. The GaAs(100) surface (Te-doped, $7.8 \times 10^{16} \text{ cm}^{-3}$) is sputtered for less than 30 min. The dashed curve is a plot of Eq. (13) assuming all terms are temperature independent.

The dashed line in Fig. 3 is obtained from Eq. (13) making the *incorrect* assumption that all terms are temperature *independent*. Despite these simplifying assumptions, the fit to the data with no adjustable parameters, is quite good.

Figure 4 shows the temperature dependence of the quasielastic peak FWHM for a Te-doped GaAs(100) sample which has been extensively sputtered and annealed (sputtering, 500 eV, $10 \mu\text{A}/\text{cm}^2$, 60 min; annealing, 850 K, 60 min). The measured full width at half maximum in Fig. 4 is significantly narrower than that of Fig. 3 at all temperatures. At 300 K the quasielastic peak has a width of 10.2 meV and therefore $\Gamma^2 = 74 \text{ meV}^2$. F is now equal to 0.03, a value approximately one-half that deduced from the experimental data in Fig. 3. ξ is then increased to over 3.1 and the barrier height [calculated from Eq. (15)] becomes an unreasonable 1.61 eV (i.e., greater than the bulk band gap).

Since, according to Eq. (13), $\Gamma^2 \sim \omega_{sp} \sim \sqrt{n}$, this discrepancy in F can be explained if one *assumes* that the effective carrier concentration in the near surface region of the sample in Fig. 4 is reduced by a factor of $\sim \frac{1}{4}$ from the bulk level. Indeed, a decrease in the near-surface free-carrier concentration is expected for GaAs as a result of sputtering and annealing.¹⁸ Extensive sputtering creates lattice imperfections (e.g., As or Ga vacancies or interstitials) in a thin layer at the surface and during the

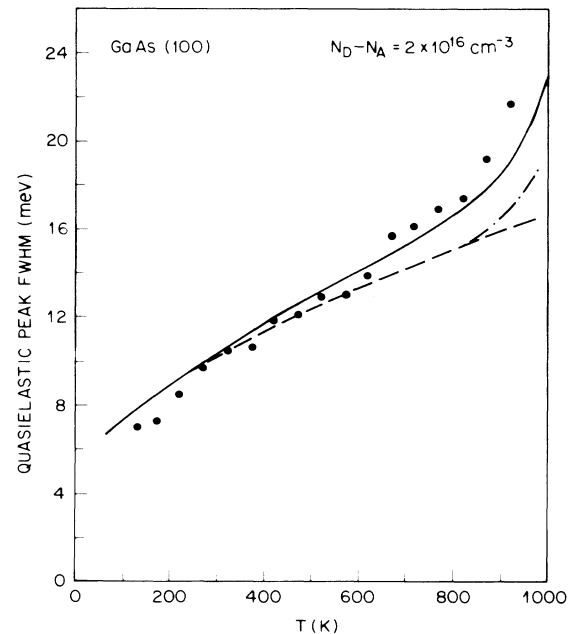


FIG. 4. The width of the quasielastic peak as a function of temperature for a GaAs(100) surface sputtered and annealed for 1 h. The near-surface free-carrier concentration is reduced to $\sim 2 \times 10^{16} \text{ cm}^{-3}$. The dashed curve is a plot of Eq. (13) assuming all terms are temperature independent. The dot-dashed curve takes into consideration the effects of thermally excited free carriers while the solid curve considers all effects including temperature induced changes in band bending (Fig. 5).

annealing process some of these will diffuse into the bulk of the semiconductor and trap free carriers. If this assumption is made, then F increases by a factor of 2 and the Fermi-level pinning position remains at 0.8 eV below the conduction-band edge (the value determined above and measured at all clean or metallized GaAs surfaces¹⁴⁻¹⁶). We also measure a similar value on samples which have been annealed for 1 h, but not sputtered. In this latter case, trace carbon and oxygen impurities remain on the surface. The presence of such impurities and/or surface defects or traps has little consequence on the results reported here due to the long probing depth of the incident electron beam⁶.

Although the theory described above is based on a three-layer model (vacuum-depletion layer-substrate), it may be applied when the acceptor point-defect concentration profile varies spatially in the near-surface region. The necessary condition, however, is that the free-carrier concentration vary *slowly* over the decay length of the surface plasmons. In the present case this requires $n(W) \approx n(2W)$. The concentration profile of point defects (in this case acceptors) after annealing can be written as

$$N_A(z) = Ae^{-(z/l)^2}, \quad (19)$$

where $A \sim 1/t$ and $l = \sqrt{4Dt}$. The diffusion constant D at the annealing temperature $T = 850$ K has been measured¹⁹ to be $D \approx 10^5$ Å²/sec. Thus after ~ 1 h of annealing, $l = 40\,000$ Å. Hence we get, with $W = 2000$ Å,

$$\frac{N_A(W) - N_A(2W)}{N_A(W)} \approx 0.01, \quad (20)$$

i.e., the carrier concentration profile varies only 1% for $W < z < 2W$ and the three-layer model can be used.

The dashed line in Fig. 4 was obtained from Eq. (13) assuming $n = 2 \times 10^{16}$ cm⁻³ ($\frac{1}{4}$ of the bulk value). Again, all of the terms in this equation were assumed to be temperature independent. For $T \gtrsim 500$ K, the experimental data show a stronger temperature dependence than predicted theoretically. Influenced by the work of Strosio and Ho,³ we initially suspected that this was due to an increase in the free-carrier concentration as a result of thermally excited electron-hole pairs (electrons excited from the valence band to the conduction band). This contribution is easily calculated, using the following equation for the concentration of free carriers⁵

$$n = \frac{1}{2} \{ (N_D - N_A) + [(N_D - N_A)^2 + 4n_i^2]^{1/2} \}, \quad (21)$$

where $N_D - N_A$ is the difference in the concentration of donor and acceptor impurities (2×10^{16} cm⁻³ is assumed in the present case) and where

$$n_i = \sqrt{N_c N_v} e^{-E_g/2k_B T}. \quad (22)$$

N_c and N_v are the effective density of states in the conduction and valence band, respectively.²⁰ The dash-dot curve in Fig. 4 shows the temperature dependence of the linewidth using this formula for the free-carrier concentration. The temperature dependence of the electron mobility ($\mu \sim 1/T$) (Ref. 5) and hence of $\bar{\omega}\tau$ ($\bar{\omega}\tau \sim 1/T$) have

also been included in this calculation. We note that the exact value of $\bar{\omega}\tau$ is not very important in the present context since varying $\bar{\omega}\tau$ by a factor of 0.5–2 only leads to small changes in F (see Fig. 2). Finally, the small, but finite, temperature dependences of ϵ_0 (Ref. 21) and m^* (Ref. 20) have been included for completeness. It is clear from Fig. 4 that thermally excited carriers give a *negligible* contribution to the linewidth for temperatures below ~ 900 K.

For GaAs, we have found that the main contribution to the width of the quasielastic scattering peak at elevated temperatures comes from the fact that as the temperature increases, the Fermi level in the bulk moves towards midgap. This is indicated in Fig. 5 and can be expressed as

$$E_c - E_F = k_B T \ln \left[\frac{N_c}{N_D - N_A} \right], \quad (23)$$

where $N_c = 4.7 \times 10^{17} (T/300 \text{ K})^{1.5}$ cm⁻³. Since the Fermi energy is pinned close to midgap at the surface, an increase in temperature will result in a decrease in band bending and hence a decreasing width of the depletion layer. A qualitatively similar conclusion was reached by Strosio and Ho on Si(111)-(7×7).³ For example, on GaAs as T increases from 300 to 900 K, W changes from 2230 Å to 1360 Å. This temperature increase results in a stronger electron-surface-plasmon coupling and therefore in a larger broadening of the quasielastic peak. Indeed, the full line in Fig. 4 has been calculated with the same parameters as above, except that ϕ and hence ξ now vary with temperature (ϕ is taken from Fig. 5). Now that all of the important contributions have been taken into effect, the agreement between theory and experiment is excellent. The effects of all of these temperature-dependent terms are much less on the sample in Fig. 3 due to its higher free-carrier concentration (the dashed curve in this figure is shifted up only slightly).

From the above it is clear that high resolution EELS is a very sensitive technique for studying variations in the

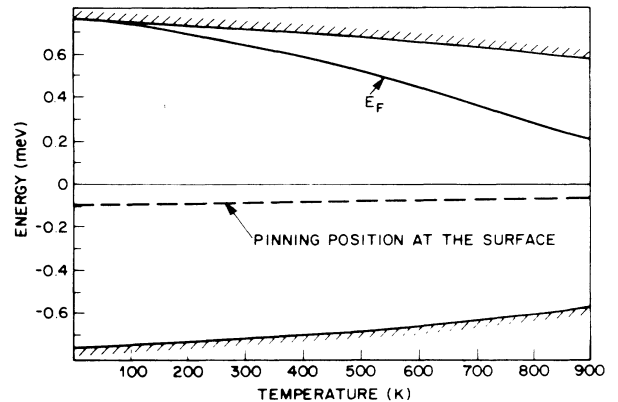


FIG. 5. The temperature dependence of the band gap and Fermi-level position for a $N_D - N_A = 2 \times 10^{16}$ doped GaAs crystal.

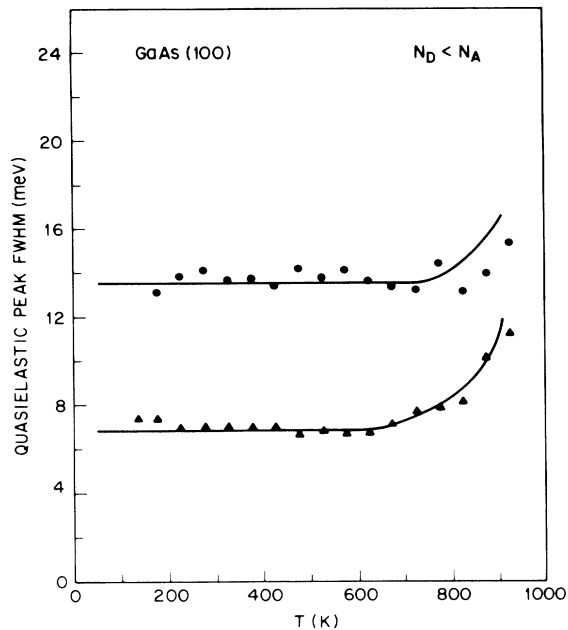


FIG. 6. The width of the quasielastic peak as a function of temperature for an extensively sputter annealed Te-doped GaAs(100) crystal, ●, and for an undoped sample, ▲. A temperature dependence is only seen above ~ 700 K. The solid curves were calculated assuming $N_D < N_A$ at 300 K.

surface free-carrier concentration of doped semiconductors. Additional examples are provided in Fig. 6. If a heavily doped GaAs sample is sputtered and annealed long enough, so many trapping point defects are generated that no free carriers are left in the near-surface region of the crystal. The quasielastic peak linewidth should then become temperature independent. That this can happen is clearly shown in the upper portion of Fig. 6. In this case a Te-doped GaAs(100) sample was sputtered for ~ 2 h and then annealed at ~ 850 K for 1 h prior to recording the EELS spectra. The resolution of the system is now on the order of 13 meV due to surface roughness induced by the long sputter-annealing cycle. A temperature dependence to the linewidth is seen only above approximately 700 K due to the effects discussed above. Similar results

are seen for undoped samples (Fig. 6, lower curve) clearly indicating that all of the free carriers in the near-surface region have been trapped. Indeed the solid curves were calculated with $N_D < N_A$ at 300 K.

V. CONCLUSIONS

Equation (13) together with Fig. 2 provide a simple, yet accurate, method for calculating the temperature-dependent linewidth of the quasielastic scattering peak from both polar and nonpolar semiconductor surfaces.

For the case of Si(111)-(7 \times 7) the band-bending and Fermi-level pinning position agree very well with the values deduced by Stroscio and Ho.³ They are also in good agreement with photoemission data. The advantage here is the simplicity with which the calculations can be done. We concluded that a negligible number of acceptor traps have been introduced beyond the depletion layer region (i.e., for $z > W$) during surface preparation (sputtering and annealing). Alternatively, the diffusion of traps at the annealing temperature is so high that n_{trap} is effectively zero in the near surface region.

For GaAs(100) we deduce, at room temperature, a Fermi-level pinning position ~ 0.8 eV below the conduction-band edge in the absence of any metal or oxide overlayer. The surface preparation (sputtering and annealing) introduces acceptor traps in the near-surface region of the GaAs crystal but does not change the Fermi-level pinning position. The trap concentration depends on how extensive the surface is sputtered and annealed but is typically in the range of 10^{16} – 10^{17} traps/cm³.

Using high-resolution EELS it may be possible to determine the diffusion coefficient of these near-surface trapping centers. By performing EELS measurements as a function of the annealing time, one can deduce the time variation of the free-carrier concentration in the near-surface region and hence draw conclusions about the diffusivity of point defects.

ACKNOWLEDGMENT

We thank G. P. Schwartz for many useful discussions and for a critical reading of the manuscript prior to publication.

¹R. Matz and H. Lüth, Phys. Rev. Lett. **46**, 500 (1981). See also A. Ritz and H. Lüth, *ibid.* **52**, 1242 (1984); H. Lüth, Surf. Sci. **168**, 773 (1986).

²L. H. Dubois and G. P. Schwartz, J. Vac. Sci. Technol. B **2**, 101 (1984); see also Phys. Rev. B **26**, 794 (1982); L. H. Dubois, G. P. Schwartz, R. E. Camley, and D. L. Mills, *ibid.* **29**, 3208 (1984).

³J. A. Stroscio and W. Ho, Phys. Rev. Lett. **54**, 1573 (1985).

⁴Even "perfect" (i.e., MBE-grown) GaAs(100) has a high density of surface states (Refs. 15 and 16).

⁵See, for example, S. M. Sze, *Physics of Semiconductor Devices* (Wiley, New York, 1981).

⁶H. Ibach and D. L. Mills, *Electron Energy Loss Spectroscopy and Surface Vibrations* (Academic, New York, 1982); A. A. Lucas and M. Sunjić, Phys. Rev. Lett. **26**, 229 (1971); W. L. Schaich, Surf. Sci. **122**, 175 (1982).

⁷B. N. J. Persson and J. E. Demuth, Phys. Rev. B **30**, 5968 (1984); J. E. Demuth and B. N. J. Persson, J. Vac. Sci. Technol. B **2**, 384 (1984).

⁸B. N. J. Persson, Phys. Rev. Lett. **50**, 1089 (1983).

⁹D. L. Mills, Surf. Sci. **48**, 59 (1975).

¹⁰A. A. Lucas and M. Sunjić, Phys. Rev. Lett. **26**, 229 (1971); W. L. Schaich, Surf. Sci. **122**, 175 (1982).

¹¹B. A. Sexton, J. Vac. Sci. Technol. **61**, 1033 (1979).

- ¹²See, for example, H. F. Wolfe, *Silicon Semiconductor Data* (Pergamon, New York, 1969).
- ¹³F. J. Himpsel, Th. Fauster, and G. Hollinger, *Surf. Sci.* **132**, 22 (1983).
- ¹⁴W. G. Spitzer and C. A. Mead, *J. Appl. Phys.* **34**, 3061 (1963).
- ¹⁵T.-C. Chiang, R. Ludeke, M. Aono, G. Landgren, F. Himpsel, and D. E. Eastman, *Phys. Rev. B* **27**, 4770 (1983).
- ¹⁶S. P. Svenson, J. Kanski, T. G. Andersson, and P. O. Nilsson, *J. Vac. Sci. Technol. B* **2**, 235 (1984).
- ¹⁷R. Z. Bachrach, R. S. Bauer, P. Chiaradia, and G. V. Hansson, *J. Vac. Sci. Technol.* **18**, 797 (1981).
- ¹⁸See, for example P. Guetin and G. Schreder, *J. Appl. Phys.* **43**, 549 (1972); M. Kawabe, N. Kanzaki, K. Masuda, and S. Namba, *Appl. Opt.* **17**, 2556 (1978); P. Kwan, K. N. Bhat, J. M. Borrego, and S. K. Ghandi, *Solid State Electron.* **26**, 125 (1983).
- ¹⁹J. S. Harris, Y. Nannichi, G. L. Pearson, and G. F. Day, *J. Appl. Phys.* **40**, 4574 (1969).
- ²⁰A detailed discussion of the temperature dependence of n_i is presented in C. D. Thurmond, *J. Electrochem. Soc.* **122**, 1133 (1975).
- ²¹J. S. Blakemore, *J. Appl. Phys.* **53**, R133 (1982).
- ²²R. A. Stradling and R. A. Wood, *J. Phys. C* **3**, L94 (1970).